OPEN ACCESS

GAVIN PUBLISHERS

Archives on Veterinary Science and Technology

Vilaplana Grosso F, et al. Arch Vet Sci Tecnol: AVST-144.

DOI: 10.29011/AVST-144/100044

Case Report

Radiographic, Ultrasonographic and Postmortem Magnetic Resonance Imaging Features of Meningoencephalocele in a Calf with Tibial Hemimelia Syndrome

Federico Vilaplana Grosso[1*], Stacy Tinkler[2], Chee Kin Lim[2], Andrea Vanderpool[3], José Ramos-Vara[3]

[1]Department of Small Animal Clinical Sciences, College of Veterinary Medicine, University of Florida, Gainesville, Florida

[2]Department of Veterinary Clinical Sciences, College of Veterinary Medicine, University of Purdue, West Lafayette, USA

[3]Department of Comparative Pathobiology, College of Veterinary Medicine, University of Purdue, West Lafayette, USA

[*]**Corresponding author:** Federico Vilaplana Grosso, Department of Small Animal Clinical Sciences, College of Veterinary Medicine, University of Florida, Gainesville, Florida, USA. Tel: +13523922226; Fax: +13528462445; Email: fvilaplanagrosso@ufl.edu

Citation: Vilaplana Grosso F, Tinkler S, Lim CK, Vanderpool A, Ramos-Vara J (2018) Radiographic, Ultrasonographic and Postmortem Magnetic Resonance Imaging Features of Meningoencephalocele in a Calf with Tibial Hemimelia Syndrome. Arch Vet Sci Tecnol: AVST-144. DOI: 10.29011/AVST-144/100044

Received Date: 09 January, 2018; **Accepted Date:** 04 May, 2018; **Published Date:** 11 May, 2018

Abstract

A 1-day-old, calf was presented for inability to stand and for evaluation of congenital anatomical and postural abnormalities. Physical examination revealed hypertrichosis, bilateral corneal edema, shortened hind limbs, an abdominal hernia and a fluctuant soft tissue swelling on the caudodorsal aspect of the head. Radiographs revealed a lucent line in the skull underlying an extracranial soft tissue swelling. Focal ultrasound (US) revealed an anechoic cystic structure contiguous with an intracranial fluid-filled cavity. Immediate postmortem magnetic resonance imaging (MRI) showed cranioschisis with two herniated meningeal sacs and focal parieto-occipital porencephaly. At necropsy, multiple intracranial, skeletal and abdominal defects were noted consistent with tibial hemimelia syndrome. Histopathology confirmed a meningoencephalocele that couldn't be differentiated from a meningocele with US nor MRI.

Keywords: Bovine; Congenital Anomaly; Magnetic Resonance Imaging (MRI); Meningoencephalocele; Tibial Hemimelia Syndrome

Introduction

The tibial hemimelia syndrome is an unusual and lethal congenital disease consisting of brain, skeletal and reproductive system defects. Calves affected by this syndrome are stillborn or die shortly after birth. This syndrome has been mainly described in Galloway calves, but can affect other breeds [10,16]. Defects included in this syndrome are: non-fusion of the Müllerian ducts in female calves, cryptorchidism in male calves, and in both sexes hypertrichosis, cranioschisis, meningocele (MC) or meningoencephalocele (MEC), internal hydrocephalus, bilateral malformation, hypoplasia or agenesis of the tibia, femur and patella, open pelvis symphysis, and abdominal hernia [10,19].

Cranioschisis is a malformation of the skull resulting in an incomplete closure of the calvarium that can lead to an opening through which the intracranial tissue can protrude. A MC is a herniation of the meninges through a cranial defect containing cerebrospinal fluid (CSF). This need to be differentiated from a MEC, in which there is also herniation of brain tissue [3]. In human medicine their differentiation is important in terms of surgical planning prognosis and surgery outcome. These defects can be congenital, as illustrated here, but can also arise after trauma [17]. Congenital MCs and MECs have been reported in calves, lambs, foals, pigs, dogs, cats and humans [2,4-8,14,15,21]. Case series in human medicine have shown that the size and content of the protruding meningeal sac has an impact on prognosis [18]. In human medicine, surgical intervention is the treatment of choice, based on the potential for recurrent meningitis, brain damage from herniation, and refractory seizures [20]. Surgical correction of MC has been previously described in calves [1,9].

A 26 kg, 1-day-old, Maine Anjou heifer calf was presented for evaluation of congenital anatomic and postural abnormalities. The calf had been unable to stand since birth. The dam had not had

any calves born with congenital malformations in the past. This calf was born a twin and the other calf was reportedly normal at birth.

At presentation, the calf was relatively bright, alert, and responsive and had a weak suckle reflex. Physical examination revealed hypertrichosis, bilateral corneal edema, shortened hind limbs, enlarged stifles with minimal range of motion, a 20 cm diameter caudal abdominal hernia and a 1.5 cm fluctuant soft tissue swelling on the caudodorsal aspect of the head that was sensitive to palpation. The rest of the physical examination was unremarkable.

Given the above clinical findings a congenital anomaly such as tibial hemimelia syndrome or bovine arthrogryposis with other congenital defects were suspected.

Orthogonal radiographs of the head and right stifle (Figure 1) were taken (Canon CXDI-80C Wireless Digital Radiography System, Melville, NY) using the settings of 1.2 mAs and 68 kVp. A 2 x 1.5 cm focal well-defined oval-shaped increase in soft tissue opacity was present at the caudodorsal aspect of the skull. A dorsoventrally oriented S-shape lucent line was present rostroventrally to the soft tissue swelling. Radiographic diagnoses included a congenital anomaly such as cranioschisis with a MC or a MEC, a skull fracture with a hematoma or swelling, and an open fontanelle with a seroma or cyst.

Figure 1. Right to left laterolateral radiographs of the head (A). An S-shaped lucent line (black arrowheads) was present at the level of the confluence between the parietal and occipital bones. A focal well-defined soft tissue swelling (white wide arrow) was present caudodorsally to the lucent line. Mediolateral and caudocranial (CdCr) radiographs of the right stifle (B, C) showing hypoplastic distal femur and proximal tibia and patella. The patella was luxated caudomedially (white arrow). On the edge of the CdCr radiograph part of an abdominal wall hernia with intestinal passage was seen (white arrowheads).

Radiographs of the right stifle showed a malformed distal femur, proximal tibia and patella. The distal femoral epiphysis was ovoid with rounded margins and without clear definition of the condyles and intercondylar fossa. The patella and the apophysis of the tibial tuberosity were small with rounded edges and displaced caudomedially. The findings were compatible with hypoplasia of the distal femur, proximal tibia and patella with concomitant medial patellar luxation and malformation of the tibial tuberosity apophysis. Additionally, there was an abdominal mass caudally to the pelvis and medially to the right stifle, containing gas-filled bowel loops and consistent with an abdominal wall hernia.

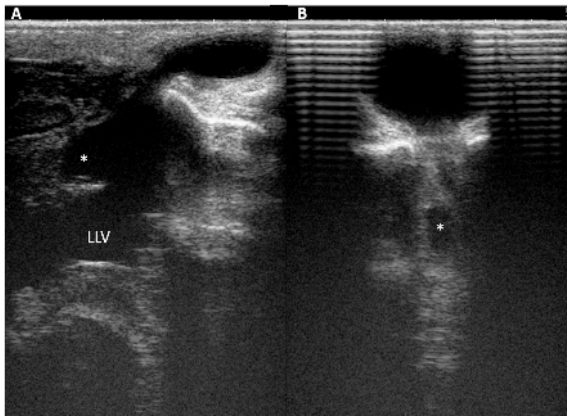

Figure 2. Sagittal (A) and transverse (B) ultrasound images of the caudodorsal calvarium. An ovoid-shaped, well-defined, thin-walled, anechoic cyst-like structure was observed within the subcutaneous tissues communicating through a calvarial defect with a large anechoic intracranial fluid-filled cavity (asterisk), presumably part of the left lateral ventricle (LLV). The rest of the LLV was ventrally to the fluid-filled cavity.

Focal ultrasound (US) of the fluctuant swelling at the caudodorsal aspect of the head was performed (Technos MPX, Esaote, Indianapolis, IN) with an 8-14 MHz linear probe (Figure 2). A 0.6 cm defect was detected at the caudodorsal aspect of the skull, traversing caudoventrally towards the junction between the left parietal and occipital bones. Through this defect, a well-defined, thin-walled (0.05 cm), oval-shaped anechoic cyst-like structure of 1.5 x 0.6 x 1.7 cm was present in the subcutaneous tissues communicating intracranially with an anechoic fluid-filled cavity. This intracranial cavity appeared contiguous with a moderately dilated left lateral ventricle. The right lateral ventricle was mildly dilated. The ultrasonographic diagnosis was cranioschisis and a MC communicating with a distended and misshapen left lateral ventricle.

Poor prognosis was given for return to ambulation for this calf and hence humane euthanasia of the calf was elected by the owner. An immediate postmortem magnetic resonance imaging (MRI) of the head was performed (1.5 T General Electric Signa, Milwaukee, WI) (Figure 3) to further characterize the lesions. The calf was positioned in sternal recumbency. Sequences included transverse

and sagittal T1-weighted (T1W) and T2-weighted (T2W) and transverse fluid attenuated inversion recovery (FLAIR) images. Repetition time and echo time were 550.0-566.6 and 10.3-16.3 ms (T1W), 3000-4050 and 100.8-106.9 ms (T2W), and 8002.0 and 128.9 ms (FLAIR). Inversion time was 2000 ms on FLAIR images. Slice thickness was 1.5-3 mm, with a 0.5-1 mm interslice gap. Field of view was 22 x 22 cm with the matrix size of 288 × 224. Two asymmetric (left: 1.5 x 1.6 x 1.5 cm and right: 0.5 cm), fluid-filled structures were noted communicating the subarachnoid space with the subcutaneous tissues through two calvarial bone defects on each side of the midline of caudodorsal skull. The cystic structures were isointense to the CSF and surrounded by a thin, well-defined T1W hyperintense, T2W hypointense and FLAIR hyperintense wall. No brain tissue was seen protruding into these cystic structures. The left parieto-occipital cerebral cortex was severely atrophied focally, leading to a large intraaxial CSF-filled cavity that communicated with the largest cystic structure. A thin rim of residual neural parenchyma was still present at that level. The rest of the cortical mantle appeared thin with widened sulci. No communication between the cystic structures and the lateral ventricles was noted. Both lateral ventricles were asymmetrically enlarged (left > right) and the rest of the ventricular system was mildly generally dilated. No evidence CSF flow obstruction was noted in the ventricular system.

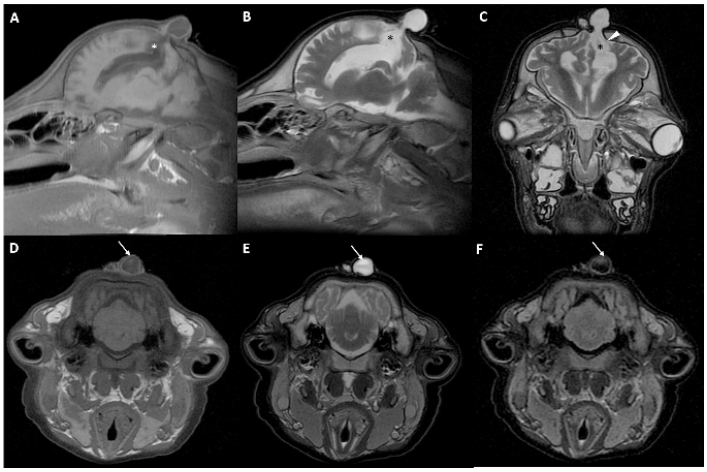

Figure 3. Immediate postmortem magnetic resonance imaging (MRI). Sagittal T1-weighted (A) and T2-weighted (B) images of the meningoencephalocele. Communication with an area of porencephaly (asterisk) was noted. Transverse oblique T2-weighted (C) image. A thin rim of left parietal cerebral cortex was present (white arrowhead). No protrusion of parenchyma into the meningeal sac was noted. A thin membrane (white arrow) was visible between the left lateral ventricle (asterisk) and the porencephalic area. Transverse T1-weighted (D), T2-weighted (E) and FLAIR (F) images of the meningoencephalocele and the other meningeal sac.

Magnetic resonance imaging findings included cranioschisis, two MCs, focal left parieto-occipital porencephaly, presumed mild generalized cortical brain atrophy and compensatory hydrocephalus ex vacuo.

At necropsy (Figure 4), two fluid-filled pouches lined by a thin membrane and covered by alopecic skin protruded through two 0.6 cm defects in the parietal bones. No macroscopic evidence of herniated brain tissue within the meningeal sacs was noted. Histologically, the larger pouch included a meningeal layer, a portion of the left lateral ventricle and the compressed overlying cerebral parenchyma (MEC). The parietal bone sutures were incompletely fused and connected by a 4 mm band of connective tissue. The medial and lateral femoral and tibial condyles were bilaterally enlarged and rounded. Both patellae were displaced medially and fused with the medial femoral condyles. The medial meniscus was bilaterally missing. Histologically, the femoral growth plates had marked expansion of the resting layer of chondrocytes occupying more than half of the growth plate thickness. The number of osteoclasts was decreased in the primary spongiosa, with retained cartilage cores in the secondary spongiosa and diaphyseal trabecular bone. Trabeculae were bordered by a reduced number of mostly flattened osteoblasts. The marrow had few hematopoietic cells.

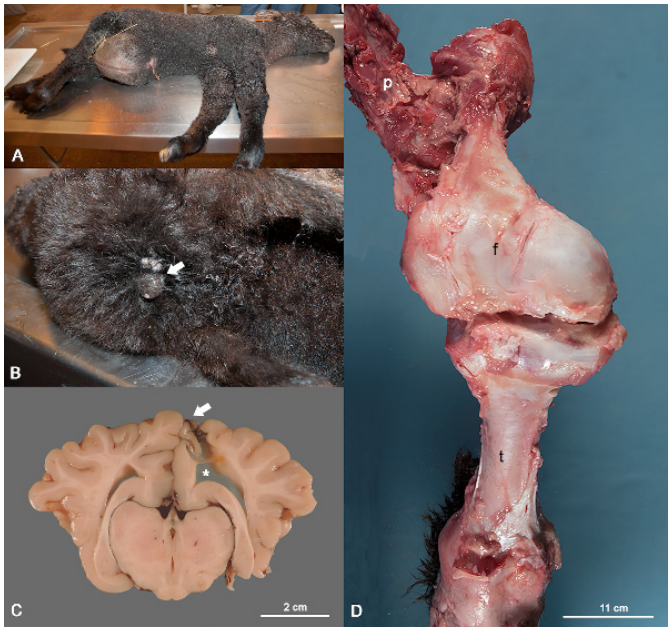

Figure 4. Postmortem photographs. (A) The caudal abdomen is markedly dilated due to the presence of a hernia. Note the shortening of the rear legs. (B) Two, skin covered, fluid-filled pouches are present in the caudodorsal aspect of the skull (arrow). C. There is dilatation of the left lateral ventricle (asterisk). The meningoencephalocele is collapsed (arrow). There is a thin membrane (above the asterisk) separating the left lateral ventricle from a smaller cavity. (D) The femur (f) is shortened and its distal epiphysis markedly distorted. The patella is fused with the medial femoral condyle. The medial and lateral condyles of the tibia (t) are enlarged. pelvic bone (p).

A large abdominal hernia was present containing segments of the small intestine, spiral colon, and omasum. The ovaries and uterus were absent and the vaginal vault ended blindly 4 cm cranial to the vulva. Histologically, the abdominal wall at this level consisted of and external lining of skin followed by connective tissue without a layer of skeletal muscle.

This calf was diagnosed with tibial hemimelia syndrome due to the presence of multiple congenital defects including cranioschisis, MEC, hydrocephalus, uterine and ovarian agenesis, bilateral dysplastic tibiae, femora, and patellae, and ventral abdominal hernia.

Radiography [1,7], US [1,15], computed tomography [12,15] and MRI [21] have been previously used for the diagnosis of MEC in calves but to the authors' knowledge this is the first detailed imaging description of MEC in a calf using radiography, US and high field MRI. The previous MRI description was performed with a low field magnet and the MEC was fronto-ethmoidal protruding into the nasal cavity. Many other cranial and vertebral malformations were diagnosed in association with the MEC in that case.

In the present patient, MRI allowed the detection of an additional subcutaneous meningeal sac that was unnoticed during the clinical, radiographic and ultrasonographic examinations.

Interestingly, histopathology of the larger subcutaneous meningeal sac contained compressed cerebral parenchyma, confirming therefore a diagnosis of MEC and not MC as believed in the US and MRI examinations. No histopathology of the other smaller meningeal sac could be performed, not allowing a histological differentiation between a MC and a MEC.

On MRI, MEC can be differentiated from MC due to the presence of hyperintense T2W and FLAIR protruded parenchyma within the meningeal sac. These intensity changes can be due to gliosis of cerebral tissue, tissue inflammation, or edema [11]. Other concurrent intracranial malformations, including porencephaly and hydrocephalus ex vacuo, were noted in this case as previously described in dogs [11]. Porencephaly has been previously described in calves but not associated with MEC [13].

MRI is a non-invasive technique that can be used in neonatal bovines for assessing congenital anomalies of the brain that could be potentially treated surgically and detection of additional abnormalities that may influence the prognosis. Although the utility of MRI in the diagnosis of MC/MEC in calves may be limited because of the cost and availability of MRI systems.

References

1. Back W, Van Den Belt AJ, Lagerweij E, Van Overbeeke JJ, Van Der Velden MA, et al. (1991) Surgical repair of a cranial meningocele in a calf. Vet Rec 128: 569-571.
2. Cho IC, Park YS, Yoo JG, Han SH, Cho SR, et al. (2015) Two cases of meningocele and meningoencephalocele in Jeju native pigs. BMC Vet Res 11: 89.
3. David JD, Proudman TW (1989) Cephaloceles: classification, pathology, and management. World J Surg 13: 349-357.
4. Dewey CW, Brewer DM, Cautela MA, Talarico LR. Silver GM, et al. (2011) Surgical treatment of a meningoencephalocele in à cat. Vet Surg 40: 473-476.
5. Hoogmoed L, Yarbrough TB, Lecouteur RA, Hornof WJ, et al. (1999) Surgical repair of a thoracic meningocele in a foal. Vet Surg 28: 496-500.
6. Jeffery N (2005) Ethmoidal encephalocoele associated with seizures in a puppy 46: 89-92.
7. Kisipan ML, Orenge CO, Gacheru DN, Ngure RM (2017) A case of cranium bifidum with meningocele in Ayrshire calf. BMC Vet Res 13: 20.
8. Kohli RN (1998) Congenital meningocele with a rare skull defect in a lamb. Aust Vet J 76: 252.
9. Kohli RN, Naddaf H (1998) Surgical treatment of meningocele in Iranian calves. Vet Rec 142: 145.
10. Lapointe JM, Lachance S, Steffen DJ (2000) Tibial hemimelia, meningocele, and abdominal hernia in shorthorn cattle. Vet Pathol 37: 508-511.
11. Lazzerini K, Gutierrez-Quintana R, José-Lopez R, McConnell F, Gonçalves R, et al. (2017) Clinical features, imaging characteristics, and long-term outcome of dogs with cranial meningeal or meningoencephalocele. J Vet Intern Med 31: 505-512.
12. Lee KJ, Yamada K, Tsuneda R, Kishimoto M, Shimizu J, et al. (2009) Clinical experience of using multidetector-row CT for the diagnosis of disorders in cattle. Vet Rec 165: 559-562.
13. Lee KJ, Yamada K, Tsuneda R, Kishimoto M, Shimizu J, et al. (2009) Imaging diagnosis-Porencephaly in a calf. Vet. Radiol Ultrasound 50: 301-303.
14. Mac Killop E (2011) Magnetic resonance imaging of intracranial malformations in dogs and cats. Vet Radiol Ultrasound 52: 42-51.
15. Ohba Y, Iguchi T, Hirose Y, Takasu M, Nishii N, et al. (2008) Computed tomography diagnosis of meningoencephalocele in a calf. J Vet Med Sci 70: 829-831.
16. Ojo SA, Guffy MM, Saperstein G, Leipold HW (1974) Tibial hemimelia in Galloway calves. J Am Vet Med Assoc 165: 548-550.
17. Rosenblatt AJ, Scrivani PV, Caserto BG, Ruby RE, Loftus JP, et al. (2014) Imaging diagnosis-Meningoencephalitis secondary to suppurative rhinitis and meningoencephalocele infection in a dog. Vet Radiol Ultrasound 55: 614-619.
18. Simpson DA, David DJ, White J (1984) Cephaloceles: treatment, outcome, and antenatal diagnosis. Neurosurgery 15: 14-21.
19. Whitlock BK, Kaiser L, Maxwell HS (2008) Heritable bovine fetal abnormalities. Theriogenology 70: 535-549.
20. Woodworth BA, Schlosser RJ, Faust RA, Bolger WE (2004) Evolutions in the management of congenital intranasal skull base defects. Arch Otolaryngol Head Neck Surg. 130: 1283-1288.
21. Zani DD, De Zani D, Morandi N, Biggi M, Belloli AG, et al. (2010) Imaging diagnosis-Split cord malformation. Vet Radiol Ultrasound 51: 57-60.